



RESEARCH ARTICLE

PRESERVING QUANTUM CORRELATIONS VIA DECOHERENCE CHANNELS
WITH MEMORY

Durgun DURAN ^{1,*} 

¹ Department of Physics, Faculty of Science and Arts, Yozgat Bozok University, Yozgat, Turkey

ABSTRACT

Considering the quantum memory channels, we study the dynamical evolutions of quantum coherence and quantum mutual information as measures of quantum correlations under the actions of different decoherence channels on some bipartite initial states. Under any quantum operation or process occurring in a noisy environment, quantum correlations exhibit behavior that does not increase due to the system interacting with its environment. We state that for such a case the decrement of quantum correlations can be improved by the suitable choice of the initial states and by adjusting the parameters. Thus quantum correlations can be partially preserved against the action of the environment. It can be shown that optimal conditions to prohibit the partial loss in quantum coherence and quantum mutual information for performing any quantum information task may be generated by the memory.

Keywords: Quantum coherence, Quantum mutual information, Quantum correlations, Quantum channels with memory

1. INTRODUCTION

Quantum correlations are the important resources in accomplishing some significant quantum computation and information tasks such as quantum teleportation, entanglement swapping, key distribution, quantum cryptography, superdense coding that cannot be achieved classically [1]. In fulfilling such a mission, conservation and sustaining of these for a long time have vital importance [2]. However, quantum correlations generally show the decreasing behavior under any quantum information process like a quantum channel (QC) in a noisy environment [3].

The loss or decrement of the correlation, called quantum decoherence, is the main obstacle in implementations of new quantum technologies based on quantum computation and information sciences [4, 5]. Therefore, it is of great importance to searching new ways to control or mitigate the decrease of correlations and make them available in information and computation technology [5, 6]. This work pursues such a purpose in the context of memory QCs [7] that are very crucial in studying noisy quantum information and computing processes.

Quantum coherence is the illustrious measure of the quantum correlations that arise from the description of the wave function of quantum systems and thus classical physics laws cannot describe it [8, 9]. Therefore, there are quantum states that have no classical counterpart due to the existence of quantum coherence and these states can only be characterized by the laws of quantum mechanics [10, 11]. Besides, these play an essential role in achieving quantum supremacy that has dramatically improved in recent years [12]. Indeed, quantum coherence is taken into account a fundamental resource within the context of quantum information processing and computation, and thus it is vital to measure and manipulate the amount of coherence present in the quantum state [13-15]. Coherence is very fragile due to veridical systems interacting with their external environment and it inevitably prone to environmental effects as information from the system flows into the environment [16]. It can be clearly said that coherence is often very hard to create, maintain, and manipulate in quantum systems. Therefore, it is

*Corresponding Author: durgunduran@hotmail.com

Received: 18.01.2021 Published: 30.08.2021

very essential and striking to create, control, sustain and preserve the quantum coherence in quantum computation and information processing.

In recent years, quantum coherence has widely been studied in many fields of quantum information and computing processes such as the extraction of work from quantum coherence in the field of quantum thermodynamics [17], quantum coherence of low-temperature thermodynamics [18, 19], quantum metrology [20, 21] and quantum algorithms [22, 23]. In addition, it attracts a great deal of interest in various fields such as energy transfer [24], quantum biology [25], photosynthesis in biological systems [26], the avian compass in migratory birds [27] and Yang-Baxter states [28].

Another quantum measure of the correlation is quantum mutual information (QMI) that characterizes the total correlations (classical and quantum) between subsystems of a bipartite system [29]. It is positive and vanishes if and only if the state of joint system is a product state.

Any quantum information process or evolution such as time evolution and quantum measurement on a quantum system are demonstrated as a QC Λ . Considering a bipartite system AB whose Hilbert spaces respectively correspond to \mathcal{H}_A and \mathcal{H}_B , a map Λ is called completely positive (CP) linear map on the set $B(\mathcal{H}_B)$ of operators living in \mathcal{H}_B . It maps the positive operators to positive ones and preserve the trace. Additionally, it maintains the positivity in all tensorial extensions [30, 31]. On the other hand, if the first system is affixed to second one then $id_A \otimes \Lambda$ is still a QC on the expanded domain for all Hilbert space of system A. id_A denotes the identity map of \mathcal{H}_A that is the simplest QC. It is noted that traits and features of the QC do not change under the convex mixing, tensorial extensions and chains of QCs with appropriate definition domains [7].

The well-known models for the action of a noisy environment on N -partite systems are the memoryless channels that can be defined as $\Lambda_N = \Lambda^{\otimes N} = \Lambda \otimes \Lambda \otimes \dots \otimes \Lambda$. If the time between consecutive actions of the QC is greater than the relaxation time of the environmental affects, one can speak of these channels [4]. In such a case, the environment backaction can be negligible at each action of the channel and the same QC Λ acts on each part of the quantum system. However, if this is not the case, the outputs or correlations obtained by the successive use of the channel on the input state are strictly depend on the previous action and these may be transmitted by the environment. In cases where the decomposition $\Lambda_N = \Lambda^{\otimes N}$ is not valid as a rule, one can speak of correlated QCs or quantum memory. Because of the continuing miniaturization of information processing devices and increasing communication rates, the attention of such quantum memory effects is inevitable [7].

QCs with memory were firstly investigated by a pioneering work to study the problem of classical capacity of them [32]. The authors studied the two consecutive actions of the depolarizing channel with correlated Markovian noise in which it can be described as a Pauli channel since it is constructed by the Pauli matrices. They showed that a higher quantity of classical information could be conveyed with maximally entangled states compared to separable ones beyond a specific threshold in the degree of quantum memory of the QC. Later, the extension of this work to the case of non-Pauli channels was investigated and similar behavior was found [33].

In this paper, we shall investigate the dynamical evolution of correlations under the two successive uses of different QCs using the quantum coherence and QMI as quantifiers of correlations of two 2-qubit systems initially prepared in a parameterized state differently from previous works. Then, we shall study the actions of two consecutive uses of different two-qubit channels called usually decoherence channels such as amplitude-damping (AD), bit-flip (BF), bit-phase-flip (BPF), phase-damping (PD) that also called phase-flip and depolarizing (DP) channels on this measure taking account of the quantum memory. Although quantum correlations decrease monotonically under the memoryless actions of these channels, by adjusting the quantum memory it can be said that the relative increments in the quantum coherence and QMI can be observed for the actions of all the channels. In the regions where correlations

can be improved, they can relatively be obtained at high values in order to be used as a resource in information and computation processes.

This study is organized as follows. In Sec. 2, the main features of the coherence and QMI that will be used in this study and quantum channels are summed up briefly. Two consecutive uses of decoherence channels on the two different inputs are realized in Sec. 3, where quantum coherence and QMI of the outputs are introduced and the central outcomes of this work are highlighted in this section. We finalize with conclusion and some remarks.

2. QUANTUM CHANNELS AND MEASURES OF QUANTUM CORRELATIONS

In this section, we start brief information about quantum coherence and QCs. To begin with, we describe the QCs and quantum coherence (relative entropy of coherence and l_1 -norm of coherence) in two subsections.

2.1. Quantum Channels

The identical and independent noises act on each part for an N –partite system of a time-ordered sequence of carries and in a memoryless case, N copies $\Lambda^{\otimes N}$ of Λ are acting. For any compound input ρ , If K_i 's that satisfy the trace-preserving property $\sum_i K_i^\dagger K_i = \mathbb{I}$ are the Kraus operators [31] of the QC Λ then

$$\Lambda^{\otimes N}(\rho) = \sum_{i_1 \dots i_N} (K_{i_1} \otimes \dots \otimes K_{i_N}) \rho (K_{i_1}^\dagger \otimes \dots \otimes K_{i_N}^\dagger), \quad (1)$$

where \mathbb{I} denotes the identity matrix.

The memory effect can be described by the correlated multi-use Λ_N of the QC Λ . In this situation, the Kraus operators of the QC are $K_{i_1 \dots i_N} = \sqrt{p_{i_1 \dots i_N}} A_{i_1} \otimes \dots \otimes A_{i_N}$ with $\sum_i p_{i_1 \dots i_N} = 1$ where $p_{i_1 \dots i_N} \geq 0$ are the probabilities of an arbitrary sequence of quantum operations carried out to information carriers when they transmit the QC. For the memoryless case, above quantum operations are independent of each other $p_{i_1 \dots i_N} = p_{i_1} p_{i_2} \dots p_{i_N}$ and $K_{i_j} = p_{i_j} A_{i_j}$. On the other hand, for a correlated QC containing the memory like forgetful channels, these operations are correlated via $p_{i_1 \dots i_N} = p_{i_1} p_{i_2|i_1} \dots p_{i_N|i_{N-1}}$ and the result of each operation depends on the previous one where $p_{i_k|i_{k-1}}$ is the conditional probability for the effect on the i_k th part of the compound quantum system.

Kraus operators for two consecutive uses of a QC with memory that quantified by the memory parameter $0 \leq \mu \leq 1$ are [32, 33] $K_{ij} = \sqrt{p_{ij}} A_i \otimes A_j$ with $p_{ij} = p_i [(1 - \mu)p_i + \mu \delta_{ij}]$ for bipartite systems. In this case, the output $\sigma = \Lambda_2(\rho)$ can be written as a convex mixture of uncorrelated and correlated parts:

$$\sigma = (1 - \mu) \sum_{i,j} K_{ij}^u \rho K_{ij}^{u\dagger} + \mu \sum_k K_k^c \rho K_k^{c\dagger}. \quad (2)$$

Here, $K_{ij}^u = \sqrt{p_i p_j} A_i \otimes A_j$ and $K_k^c = \sqrt{p_k} A_k \otimes A_k$. From Equation (2) says that with probability μ the QC acts on both information carriers with the same quantum operator A_k , whereas it independently acts on the carriers with probability $1 - \mu$. Physically, μ is obtained by the relaxation or correlation time of the QC when one of the carrier traverses it [30].

2.2. Quantum Coherence

Before moving on to the definition of coherence, we will give a few useful mathematical definitions for this topic.

Definition: Let \mathcal{H} be a d –dimensional Hilbert space. Let us fix a basis $\{|i\rangle\}_{i=1}^d$ of vectors in \mathcal{H} . A quantum state π is called incoherent if it can be represented as follows

$$\pi = \sum_i \pi_i |i\rangle\langle i|. \quad (3)$$

For a fixed basis $\{|i\rangle\}_{i=1}^d$, the set of incoherent states is denoted as $\mathcal{I} = \{\pi = \sum_i p_i |i\rangle\langle i|\}$.

Recently, a recipe for the qualification of the coherence has been supplied by taking into consideration coherence as a quantum resource [8]. In this study, the following set of criteria (so-called Baumgratz et al. criteria) has been proposed that each potential coherence quantifier (C) should satisfy:

- (1) Coherence has the non-negativity behavior: $C(\rho) \geq 0$ and ρ is an incoherent state if and only if the equality holds.
- (2a) Monotonicity: C has the non-increasing behavior under the actions of CP and trace-preserving (TP) incoherent operations, i.e., $C(\Phi(\rho)) \leq C(\rho)$, where Φ is any CPTP incoherent operation.
- (2b) Strong monotonicity: $\sum_i q_i C(\rho_i) \leq C(\rho)$, where $\rho_i = (K_i \rho K_i^\dagger)/q_i$ are post-measurement states. The probabilities are given by $q_i = \text{Tr}(K_i \rho K_i^\dagger)$, and K_i 's are incoherent Kraus operators.
- (3) Convexity: C has the non-increasing behavior under any convex mixture, i.e.

$$\sum_i p_i C(\rho_i) \leq C\left(\sum_i p_i \rho_i\right). \quad (4)$$

Now, we can introduce the two types of quantum coherence, separately.

As a measure of quantum correlations, we firstly give the relative entropy of coherence living in a quantum state symbolized by a bipartite matrix ρ_{AB} or shortly ρ . It is defined as [8]

$$C_r(\rho) = S(\rho_{diag}) - S(\rho), \quad (5)$$

where $S(\rho) = -\text{Tr} \rho \log \rho$ is the von Neumann entropy of ρ and if λ_i are the eigenvalues of ρ then it can be expressed as $S(\rho) = -\sum_i \lambda_i \log \lambda_i$. ρ_{diag} denotes the diagonalized form of ρ . It is noted that C_r is a basis-dependent quantity. C_r has a physical importance because of its similarity to the relative entropy of entanglement in form. It physically states the best rate of the distilled maximally coherent states that may be made by incoherent operations within the asymptotic limit of the many copies of ρ [34]. The experimental measurement of $C_r(\rho)$ may interestingly be achieved without using full quantum state tomography [35].

Secondly, the l_1 -norm of coherence in which we focus on in this paper is given by [8]

$$C_{l_1}(\rho) = \sum_{i \neq j} |\rho_{ij}|, \quad (6)$$

where ρ_{ij} denotes the matrix elements of ρ . l_1 -norm of coherence, which like C_r is basis dependent, is currently not known to have any analog in the entanglement resource theory [13].

Interestingly, for any d –dimensional mixed state, it has been proved that $C_{l_1}(\rho) \geq C_r(\rho)/\log_2 d$ and conjectured that $C_{l_1}(\rho) \geq C_r(\rho)$ for all states [14].

2.3. Quantum Mutual Information

QMI as a measure of total correlations living in a bipartite quantum system that can be divided into parts A and B is defined as

$$I(\rho_{AB}) = S(\rho_A) + S(\rho_B) - S(\rho_{AB}), \quad (7)$$

where $\rho_{A(B)} = \text{Tr}_{B(A)}\rho_{AB}$ is the reduced density matrix of the system AB and $S(\rho_i) = -\text{Tr}\rho_i \log_2 \rho_i$ is the von Neumann of the subsystem ($i = A, B$). The entropy of total system AB is also defined as $S(\rho_{AB}) = -\text{Tr}\rho_{AB} \log_2 \rho_{AB}$. QMI has a non-increasing behavior under any quantum channel [1] and for two-qubits, we have $0 \leq I(\rho_{AB}) \leq 2$.

3. TWO-USE ACTIONS OF THE QUANTUM CHANNELS WITH MEMORY

In this section, we investigate the successive action of AD, PD, BF, BPF and DP channels, denoted respectively by Λ^{AD} , Λ^{PD} , Λ^{BF} , Λ^{BPF} and Λ^{DP} on two different 2-qubit input states and focus on calculations of quantum coherence and QMI of the corresponding outputs.

The number of Kraus operators of the first four channels are two and each of them typically depends on a parameter represented by $0 \leq p \leq 1$ that represents the decoherence parameter of the channel. The last channel Λ^{DP} has the full rank where there are four Kraus operators. The Kraus operators of these channels are given in Table 1. We first fix two different input states and found their values for the initial states of quantum coherence and QMI. Then, we investigate the dynamics of them for the outputs obtained by help of the Equations (2), (6) and (7) taking account of the quantum memory.

3.1. Initial Values of the Quantum Coherence and QMI

Firstly, we fix the two-qubits isotropic state as an input

$$\rho_{AB}^{(1)} = (1-x)\frac{\mathbb{I}}{4} + x|\Psi^+\rangle\langle\Psi^+|, \quad (8)$$

where $x \in [0,1]$ is the mixing or state parameter and $|\Psi^+\rangle = (|00\rangle + |11\rangle)/\sqrt{2}$ is the Bell state in the computational basis $\{|00\rangle, |01\rangle, |10\rangle, |11\rangle\}$ [1]. The states $|0\rangle$ and $|1\rangle$ correspond to respectively spin-up and spin-down states and given by as follows in the matrix form

$$|0\rangle = \begin{pmatrix} 1 \\ 0 \end{pmatrix}, \quad |1\rangle = \begin{pmatrix} 0 \\ 1 \end{pmatrix}. \quad (9)$$

The initial value of the l_1 -norm of coherence, shortly coherence, for this state from Equation 6 is found to be $C_{l_1}(\rho_{AB}^{(1)}) = x$.

On the other hand, the spectra of the reduced density matrices ρ_A and ρ_B are the same and given by $\{1/2, 1/2\}$. It is noted that the first three eigenvalues of the isotropic state $\rho_{AB}^{(1)}$ for two-qubits are the same and equal to $(1-x)/4$ and the last eigenvalue is $(1+3x)/4$. In this situation, from Equation (7) QMI for this initial state is obtained as follows

$$I(\rho_{AB}^{(1)}) = 2 + 3\left(\frac{1-x}{4}\right)\log\left(\frac{1-x}{4}\right) + \left(\frac{1+3x}{4}\right)\log\left(\frac{1+3x}{4}\right). \quad (10)$$

The initial values of the coherence and QMI are depicted in Figure 1 versus the parameter x . Evidently, the coherence linearly depends on the mixing parameter and it naturally attains its maximum value for the maximum value of the $x = 1$ in which the initial state reduces to a maximally entangled pure state, namely a Bell state $|\Psi^+\rangle$. Similarly, QMI increases with the increasing values of the parameter x and takes place its maximum value for $x = 1$ as expected.

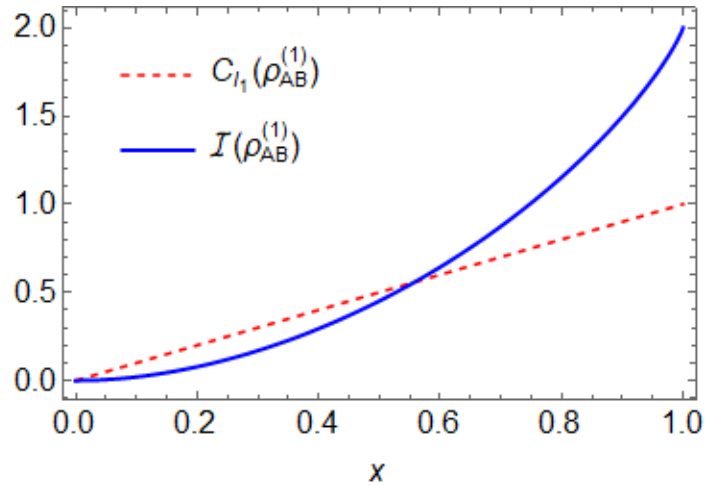


Figure 1. Plots of the coherence and QMI for the input state given by Equation 8.

Secondly, we consider the input state

$$\rho_{AB}^{(2)} = x|\Phi^-\rangle\langle\Phi^-| + \frac{1-x}{2}(|\Phi^+\rangle\langle\Phi^+| + |\Psi^+\rangle\langle\Psi^+|), \quad (11)$$

where $|\Phi^\pm\rangle = (|01\rangle \pm |10\rangle)/\sqrt{2}$ denotes the Bell states [1]. For this input state, the coherence and QMI are obtained from Equations (6) and (7) as follows

$$C_{l_1}(\rho_{AB}^{(2)}) = \frac{1}{2}(|1-3x| + |1-x|), \quad (12a)$$

$$I(\rho_{AB}^{(2)}) = 1 + x - h(x), \quad (12b)$$

respectively. Here, $h(x) = -x \log x - (1-x) \log(1-x)$ denotes the binary entropy.

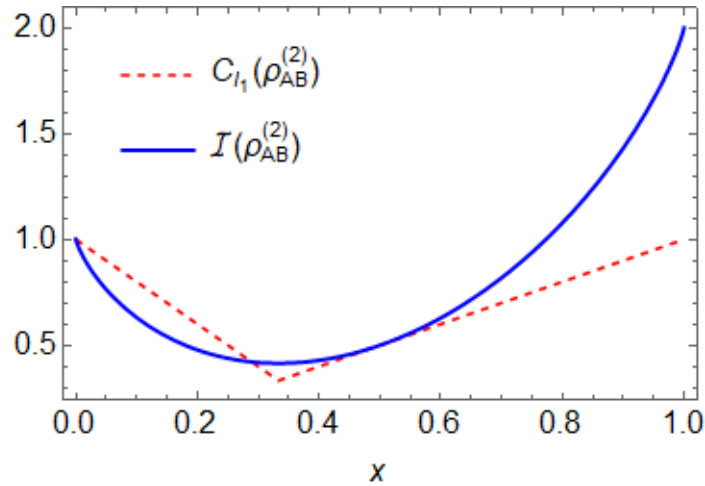


Figure 2. Plots of the coherence and QMI for the second input state given by Equation 11.

Figure 2 shows the behaviors of the coherence and QMI versus the parameter x for the second initial state $\rho_{AB}^{(2)}$. For the range of $x \leq 1/3$, coherence linearly decreases and takes its minimum value for the $x = 1/3$ whereas the other ranges of the parameter it linearly increases with the parameter x and attains its maximum for $x = 1$ similar to the previous case. It can be seen that the coherence takes place its maximum values for the smallest and the largest values of x as expected in which the input state reduced to the Bell state and a mixture of the two Bell states with equal probability, respectively. It can obviously be concluded that for different input states, coherence shows different behavior depending on the mixing

parameter x . Differently from previous one, QMI is equal to 1 for the value of $x = 0$ while it attains its maximum values for $x = 1$.

3.2. Actions of the Decoherence Channels with Memory for the Input State $\rho_{AB}^{(1)}$

Henceforward, under the actions of decoherence channels with memory on the inputs $\rho_{AB}^{(i)}$ ($i = 1,2$), for outputs $\sigma_{AB}^{(i)}$, l_1 -norm of coherence and QMI will be denoted by $C_X(\sigma_{AB}^{(i)})$ and $I^X(\sigma_{AB}^{(i)})$ with $X = AD, PD, BF, BPF, DP$ respectively. Now, we consider the actions of decoherence channels with memory on two input states, separately.

Table 1. Kraus operators of the decoherence channels with memory where p represents the decoherence parameter

Channels	Kraus Operators	
	Uncorrelated	Correlated
AD	$K_{ij}^u = A_i \otimes A_j; \quad i, j = 0,1$ $A_0 = \begin{pmatrix} \sqrt{1-p} & 0 \\ 0 & 1 \end{pmatrix}, \quad A_1 = \begin{pmatrix} 0 & 0 \\ \sqrt{p} & 0 \end{pmatrix}$ $p = 1 - \exp(-\gamma t)$	$K_0^c = \text{diag}(\sqrt{1-p}, 1, 1, 1)$ $K_1^c = \begin{pmatrix} 0 & 0 & 0 & 0 \\ 0 & 0 & 0 & 0 \\ 0 & 0 & 0 & 0 \\ \sqrt{p} & 0 & 0 & 0 \end{pmatrix}$
BF	$K_{ij}^u = \sqrt{P_i P_j} \sigma_i \otimes \sigma_j; \quad i, j = 0,1$ $P_0 = 1 - p, \quad P_1 = p$	$K_k^c = \sqrt{P_k} \sigma_k \otimes \sigma_k; \quad k = 0,1$ $\sigma_0 = \begin{pmatrix} 1 & 0 \\ 0 & 1 \end{pmatrix}, \quad \sigma_1 = \begin{pmatrix} 0 & 1 \\ 1 & 0 \end{pmatrix}$
BPF	$K_{ij}^u = \sqrt{P_i P_j} \sigma_i \otimes \sigma_j; \quad i, j = 0,2$ $P_0 = 1 - p, \quad P_2 = p$	$K_k^c = \sqrt{P_k} \sigma_k \otimes \sigma_k; \quad k = 0,2$ $\sigma_0 = \begin{pmatrix} 1 & 0 \\ 0 & 1 \end{pmatrix}, \quad \sigma_2 = \begin{pmatrix} 0 & -i \\ i & 0 \end{pmatrix}$
PD	$K_{ij}^u = \sqrt{P_i P_j} \sigma_i \otimes \sigma_j; \quad i, j = 0,3$ $P_0 = 1 - p, \quad P_3 = p$	$K_k^c = \sqrt{P_k} \sigma_k \otimes \sigma_k; \quad k = 0,3$ $\sigma_0 = \begin{pmatrix} 1 & 0 \\ 0 & 1 \end{pmatrix}, \quad \sigma_3 = \begin{pmatrix} 1 & 0 \\ 0 & -1 \end{pmatrix}$
DP	$K_{ij}^u = \sqrt{P_i P_j} \sigma_i \otimes \sigma_j; \quad i, j = 0,1,2,3$ $P_0 = 1 - p, \quad P_1 = P_2 = P_3 = p/3$	$K_k^c = \sqrt{P_k} \sigma_k \otimes \sigma_k; \quad k = 0,1,2,3$

Case 1: Amplitude-damping channel with memory

Amplitude-damping channel characterizes the spontaneous emission and represents the dissipative interaction between system and the environment. Note that the parameter $p = 1 - \exp(-\gamma t)$ where γ represents the decay rate. From Equation 2 and Table 1, under the consecutive uses of this channel, the matrix elements of the output $\sigma_{AB}^{(1)}$ corresponding to input state $\rho_{AB}^{(1)}$ given by Equation 7 are calculated in two-qubit computational basis $\{1 = |00\rangle, 2 = |01\rangle, 3 = |10\rangle, 4 = |11\rangle\}$ as follows

$$\sigma_{11}^{(1)} = 1 - \sigma_{22}^{(1)} - \sigma_{33}^{(1)} - \sigma_{44}^{(1)},$$

$$\sigma_{22}^{(1)} = \sigma_{33}^{(1)} = \frac{1}{4} \{1 - x - p(1 - \mu)[p - (2 - p)x]\},$$

$$\sigma_{44}^{(1)} = \frac{1}{4} \{(1+x)[(1-p)^2 + (3-p)p\mu]\},$$

$$\sigma_{14}^{(1)} = \sigma_{41}^{(1)} = \frac{1}{4} \{2x[\alpha - \mu(1 - \sqrt{1-p})]\},$$

where $\alpha = 1 - p(1 - \mu)$. The other elements of the output $\sigma_{AB}^{(1)}$ are zero. Thus, the coherence can be written from Equation 6 as

$$C_{AD}(\sigma_{AB}^{(1)}) = |x[\alpha - \mu(1 - \sqrt{1-p})]|. \quad (13)$$

The explicit form of QMI for this output is more complicated and not reported here but the behavior of it is plotted in Figure 4.

Case 2: Phase-damping channel with memory

The phase-damping channel that is a unital channel $\Lambda^{PD}(\mathbb{I}_{\mathcal{H}_A}) = \mathbb{I}_{\mathcal{H}_B}$ describes a quantum noise with loss of quantum phase information but not loss of energy. Again, from Equation 2 and Table 1 the output state can be calculated under the two consecutive uses of this channel and is not reported here for the fluency of the article. In this situation, the coherence and QMI are found to be

$$C_{PD}(\sigma_{AB}^{(1)}) = |x\alpha|, \quad (14a)$$

$$I^{PD}(\sigma_{AB}^{(1)}) = 2 + \frac{1}{4} \left\{ (1+x) \log[(1+x)^2 - 4\alpha^2 x^2] - 2\alpha x \log \frac{1+x-2\alpha x}{1+x+2\alpha x} \right\} + \frac{1-x}{2} \log \frac{1-x}{2}, \quad (14b)$$

respectively.

Case 3: Bit-flip channel with memory

Bit-flip channel that is important in the quantum error correction flips the state of a qubit from $|0\rangle$ to $|1\rangle$ (and vice versa) with probability $1-p$. The coherence and QMI can again be calculated as

$$C_{BF}(\sigma_{AB}^{(1)}) = |x(1-\beta)| + \frac{1}{4} |x\beta|, \quad (15a)$$

$$I^{BF}(\sigma_{AB}^{(1)}) = 2 + \frac{1-x}{2} \log \frac{1-x}{2} + \frac{1}{4} [1+x(3+4\beta)] \log \frac{1}{4} [1+x(3+4\beta)] + \frac{1}{4} \left[1-x \left(1 - \frac{3\beta}{2} \right) \right] \log \frac{1}{4} \left[1-x \left(1 - \frac{3\beta}{2} \right) \right] + \frac{1}{4} \left[1-x \left(1 - \frac{5\beta}{2} \right) \right] \log \frac{1}{4} \left[1-x \left(1 - \frac{5\beta}{2} \right) \right], \quad (15b)$$

where $\beta = 2p(1-p)(1-\mu)$.

Case 4: Bit-phase-flip channel with memory

As the name indicates, the bit-phase-flip channel is a combination of a phase-flip and a bit-flip, since $\sigma_2 = i\sigma_1\sigma_3$ where σ_i 's are the Pauli matrices. Similar to the previous cases the outputs can be calculated under the two consecutive uses of this channel from Table 1 and Equation 2. Thus, the coherence and QMI for this output can respectively be written as follows

$$C_{BPF}(\sigma_{AB}^{(1)}) = |x(1-\beta)| + \frac{1}{4} |x\mu\beta|, \quad (16a)$$

$$\begin{aligned}
 I^{BPF}(\sigma_{AB}^{(1)}) &= 2 + \frac{1-x}{2} \log \frac{1-x}{2} + \frac{1}{4} [1 + x(3 + 4\beta)] \log \frac{1}{4} [1 + x(3 + 4\beta)] \\
 &+ \frac{1}{4} \left\{ 1 - x \left[1 - \frac{\beta(4 - \mu)}{2} \right] \right\} \log \frac{1}{4} \left\{ 1 - x \left[1 - \frac{\beta(4 - \mu)}{2} \right] \right\} \\
 &+ \frac{1}{4} \left\{ 1 - x \left[1 - \frac{\beta(4 + \mu)}{2} \right] \right\} \log \frac{1}{4} \left\{ 1 - x \left[1 - \frac{\beta(4 + \mu)}{2} \right] \right\}. \tag{16b}
 \end{aligned}$$

It is noted that Equations 16 are similar to the previous one. The second term in RHS of Equation (16a) contains a memory factor μ differently from the second term in RHS of Equation (15a). Similar observations can also be made for Equations (15b) and (16b).

Case 5: Depolarizing channel with memory

The depolarizing channel is an important type of quantum noise. Imagine we take a single qubit, and with probability p that qubit is depolarized. That is, it is replaced by the completely mixed state $\mathbb{I}/2$. With probability $1 - p$ the qubit is left unchanged. For the action of this channel with the abbreviation $\gamma = 9 - 8p(3 - 2p)(1 - \mu)$, the coherence and QMI are obtained as

$$C_{DP}(\sigma_{AB}^{(1)}) = \frac{1}{9} |x\gamma|, \tag{17a}$$

$$I^{DP}(\sigma_{AB}^{(1)}) = 2 + \frac{1}{12} (3 + x\gamma) \log \frac{1}{12} (3 + x\gamma) + \frac{1}{12} (9 - x\gamma) \log \frac{1}{36} (9 - x\gamma). \tag{17b}$$

For all the actions of the decoherence channels with memory, the behaviors of the coherence are depicted in Figure 3 concerning the decoherence parameter p and the state parameter x for some fixed values of μ . In Figures 3(a), (b) and (c), the coherence increases with the increasing value of the memory parameter μ . For the smallest values of x and the largest value of p , it attains its minimum value in Figure 3(a) whereas as x increases in which the initial state is reduced to a Bell state for $x = 1$, so does it for the small value of p . In Figure 3(b) that corresponds to the action of the PD channel, the coherence increases with the increasing values of x . Additionally, although the information in the system partially decreases under any quantum operation such as QC, as the memory parameter changes from the memoryless case $\mu = 0$ to the long-term memory $\mu = 1$ the coherence shows an increasing behavior. For the action of the BF channel, it has an interesting behavior that demonstrates that at the largest and smallest values of p the coherence reaches its maximum value for $\mu = 1$. It can be shown that when $\mu = 1$ the value of coherence coincides with the initial value of it for all plots except the action of the AD channel. Another interesting result is that in Figure 3(d) and (e), coherence partially increases with the memory parameter μ . For some small values of p , approximately $p \leq 1/3$, as memory increases, the coherence also increases. However, it also attains its maximum value at $\mu = 0$ and $\mu = 1/2$ for both the largest and smallest values of p in Figure 3(d). In Figure 3(e), differently from (d) the coherence takes its minimum value for $\mu = 0$ and again when $\mu = 1$, it is the maximum for some values of $p \leq 3/4$. On the other hand, in the cases of $p > 3/4$ it reaches the maximum at $\mu = 1/2$.

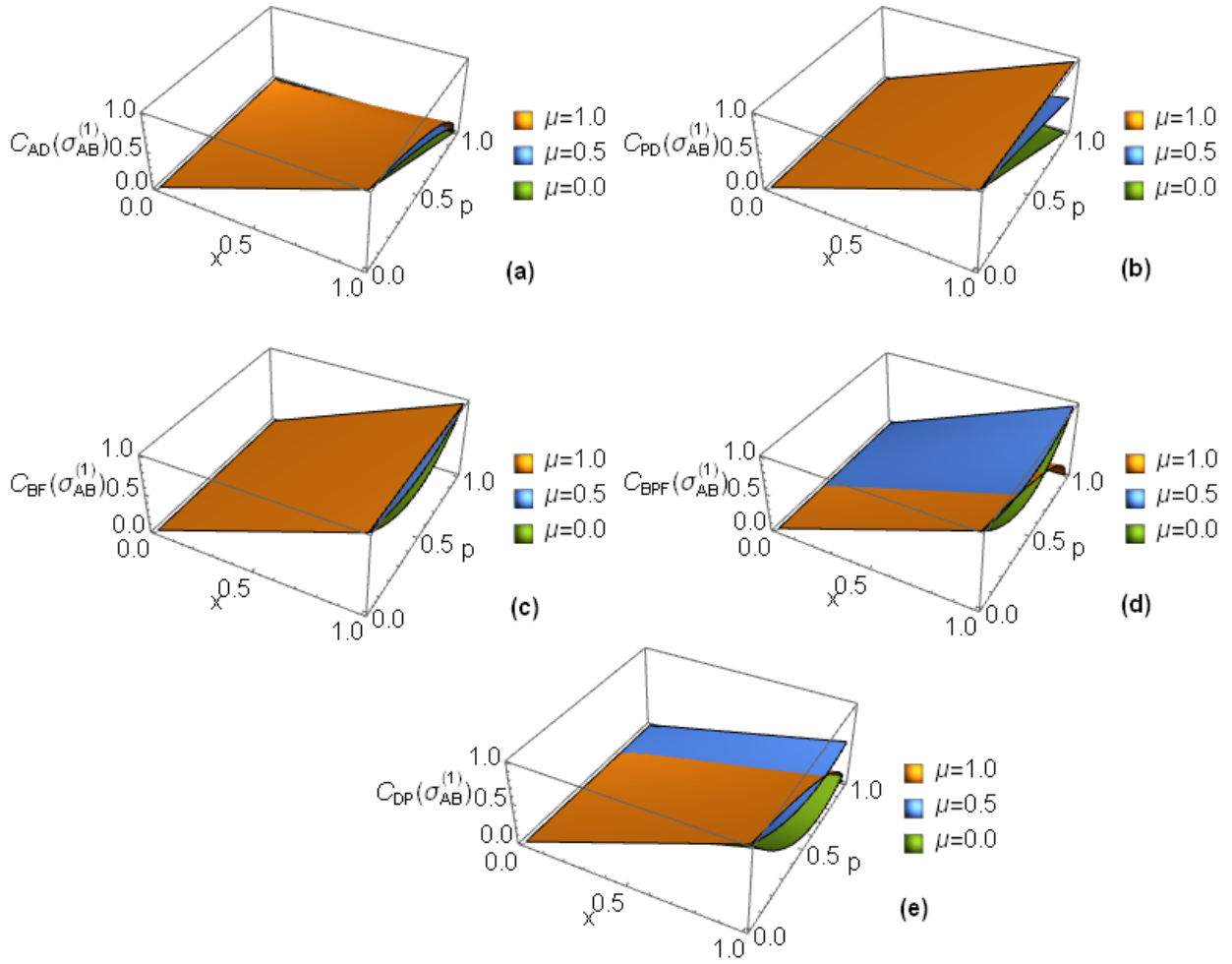


Figure 3. Plots of the coherence versus parameters p and x for outputs corresponding to the input $\rho_{AB}^{(1)}$. For all plots, the quantum memory is relatively enhanced the loss of quantum correlations. In (d) and (e), the coherence increases with the large values of the parameter p . For long-term memory $\mu = 1$, the coherence is maximum for the large values of x irrespective of p in (b) and (c). On the other hand, it monotonically decreases with the decreasing values of p in (a).

Under the actions of all decoherence channels on the first input state, the behaviors of QMIs for the corresponding outputs are plotted in Figure 4 with respect to parameters x and p for some fixed μ . In Figure 4(a), QMI naturally takes its maximum value for the largest value of x and the smallest value of p . For the increasing values of x and the intermediate values of p , it can be relatively enhanced when the channel changes from the memoryless case $\mu = 0$ to long-term memory $\mu = 1$. This result applies to other figures as well. In Figure 4(b), (c) and (e), QMI attains the maximum values for the long-term memory. On the other hand, for the memoryless case $\mu = 0$ and long-term memory $\mu = 1$, the values of QMI of the output under the actions of the BPF channel on the input coincide in Figure 4(d). It is concluded that for action of this channel, the quantum memory does not influence the behavior of the QMI.

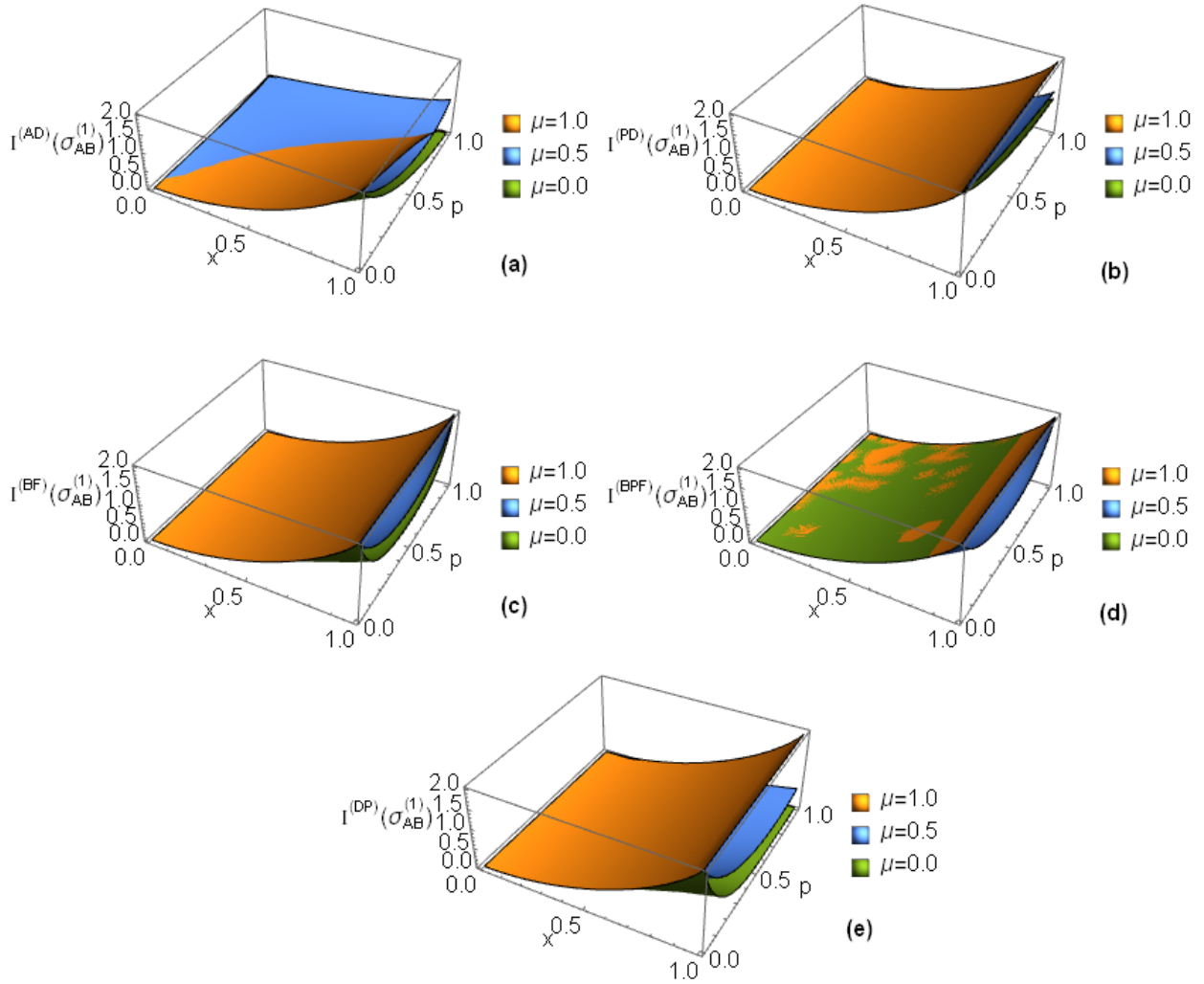


Figure 4. Plots of QMI versus parameters p and x for outputs under the decoherence channels on input state $\rho_{AB}^{(1)}$. In (b), (c), (d) and (e), the QMI increases with the increasing values of the parameter x for all values of p in the case of the long-term memory $\mu = 1$, and attains its maximum values for $x = 1$. In (a), it is the maximum for the largest value of x and the smallest value of p .

For the memoryless actions of the channels that are not reported here, the coherence has a decreasing behavior as expected. On the other hand, for $\mu = 0$, the observation coincides the memoryless case. It is well known that quantum correlations decrease under any quantum operation. However, it can be observed that this loss of correlations can generally be mitigated via quantum memory channels as used here.

3.3. Actions of the Decoherence Channels with Memory for the Input State $\rho_{AB}^{(2)}$

In this section, we give only the coherence measure for the outputs under the actions of decoherence channels with memory on the input state $\rho_{AB}^{(2)}$ given by Equation 11. Parallel to the previous section, the coherence can be calculated from Equation 6 for actions of all decoherence channels as follows

$$C_{AD}(\sigma_{AB}^{(2)}) = \frac{1}{2} \{ |(1-x)[\alpha - (1-\sqrt{1-p})\mu]| + |(1-3x)\alpha| \}, \quad (18a)$$

$$C_{PD}(\sigma_{AB}^{(2)}) = \frac{1}{2}[|(1-x)\alpha| + |(1-3x)\alpha|], \quad (18b)$$

$$C_{BF}(\sigma_{AB}^{(2)}) = \frac{1}{2}[|1-x(1+2\beta)| + |1-x(1+2\beta)|], \quad (18c)$$

$$C_{BPF}(\sigma_{AB}^{(2)}) = \frac{1}{2}[|1-x-\alpha(1-2x)| + |1-3x-\alpha(1-2x)|], \quad (18d)$$

$$C_{DP}(\sigma_{AB}^{(2)}) = \frac{1}{18}[|(1-x)\gamma| + |(1-3x)\gamma|]. \quad (18e)$$

Similarly, QMIs for all outputs can be calculated from Equation 7 as

$$I^{PD}(\sigma_{AB}^{(2)}) = 2 + \frac{1}{4}\left\{\frac{\beta}{2}\log\frac{\beta}{8} + (1-x)(1+\alpha)\log\frac{1}{4}(1-x)(1+\alpha) + [2(1-x) - \delta]\log\frac{1}{4}[2(1-x) - \delta] + (4x + \delta)\log\frac{1}{4}(4x + \delta)\right\}, \quad (19a)$$

$$I^{BF}(\sigma_{AB}^{(2)}) = 2 + (1-x)\log\frac{1-x}{2} + \beta x \log \beta x + x(1-\beta)\log x(1-\beta), \quad (19b)$$

$$I^{BPF}(\sigma_{AB}^{(2)}) = 2 + [x + \beta(1-3x)]\log[x + \beta(1-3x)] + \frac{1}{2}\left\{(1-x)(1-\beta)\log\frac{1}{2}(1-x)(1-\beta) + \beta(1-x)\log\frac{\beta(1-x)}{2} + [(1-x) - \beta(1-3x)]\log\frac{1}{2}[(1-x) - \beta(1-3x)]\right\}, \quad (19c)$$

$$I^{DP}(\sigma_{AB}^{(2)}) = 2 + \frac{1}{36}\left\{(9-\gamma)\log\frac{(9-\gamma)}{36} + 2[(9+\gamma)(1-2x)]\log\frac{1}{36}[(9+\gamma)(1-2x)] + [36x + (9-\gamma)(1-4x)]\log\frac{1}{36}[36x + (9-\gamma)(1-4x)]\right\}, \quad (19d)$$

where $\delta = p(1-3x)(1-\mu)$. Since $I^{AD}(\sigma_{AB}^{(2)})$ is more complicated it is not again reported here.

Figure 5 displays the behavior of the coherence of the outputs $\sigma_{AB}^{(2)}$ under the action of decoherence channels with memory on the input $\rho_{AB}^{(2)}$. In Figure 5(a), (b) and (e), the coherence takes its maximum value for the long-term memory $\mu = 1$. Interestingly, while the coherence coincides for all values of the memory parameter μ at $x \leq 1/3$ in Figure 5(c) and attains its maximum irrespective of p , it happens for $x > 1/3$ in Figure 5(d). On the other hand, for $x > 1/3$ the coherence increases with the increasing values of μ in Figure 5(c) whereas it manifests itself for the values of $x \leq 1/3$ in Figure 5(d). For all the plots, the value of the coherence is reduced to that of the initial state given by $C_{l_1}(\rho_{AB}^{(2)}) = (|1-3x| + |1-x|)/2$ for the long-term memory $\mu = 1$. Although the quantum correlations generally decrease by the actions of any QC, the partial loss, preservation and maintaining of correlations for a long duration can be controlled via quantum memory for all the plots in the study of any quantum information processes.

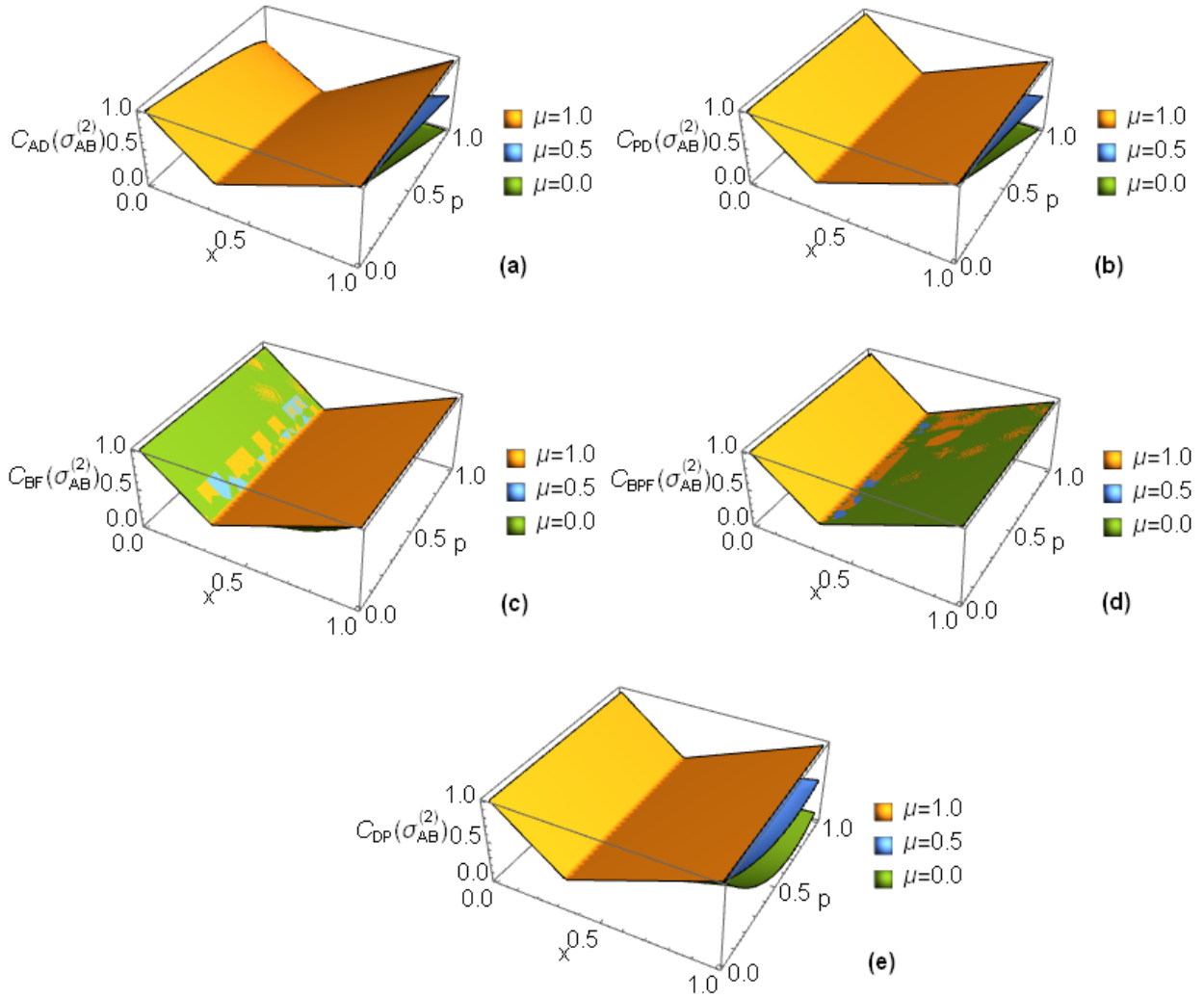


Figure 5. Plots of the l_1 -norm of coherence versus parameters p and x for outputs corresponding to the input $\rho_{AB}^{(2)}$ for some fixed μ . In the case of the long-term memory $\mu = 1$, the coherence has its maximum value for all plots. The memory is obviously improved the quantum correlations. In (c), whereas the coherence monotonically decreases for the range of $0 < x < 1/3$, it increases for $x > 1/3$. The opposite behavior is observed in (d).

The behaviors of QMIs for the second output state under the actions of decoherence channels are depicted in Figure 6 for some values of the memory parameter μ . Differently from previous one, under the action of AD channel, QMI attains its maximum values for long-term memory $\mu = 1$ independently of the other parameters x and p in Figure 6(a). Additionally, QMI is the maximum for the all plots when the memory is maximum. In Figure 6 (d), the values of it coincide for the values of $\mu = 0$ and $\mu = 1$. On the other hand, QMI increases for the long-term memory $\mu = 1$ with increasing values of p , although the decoherence parameter p is expected to lead to a decrease in quantum correlations in all plots. Evidently, the memory and the selection of different initial states, provides relative improvements in quantum correlations. In view of above observation, this implies that the decrements of the quantum correlations can be relatively enhanced by the quantum memory channels and by choosing optimal input states.

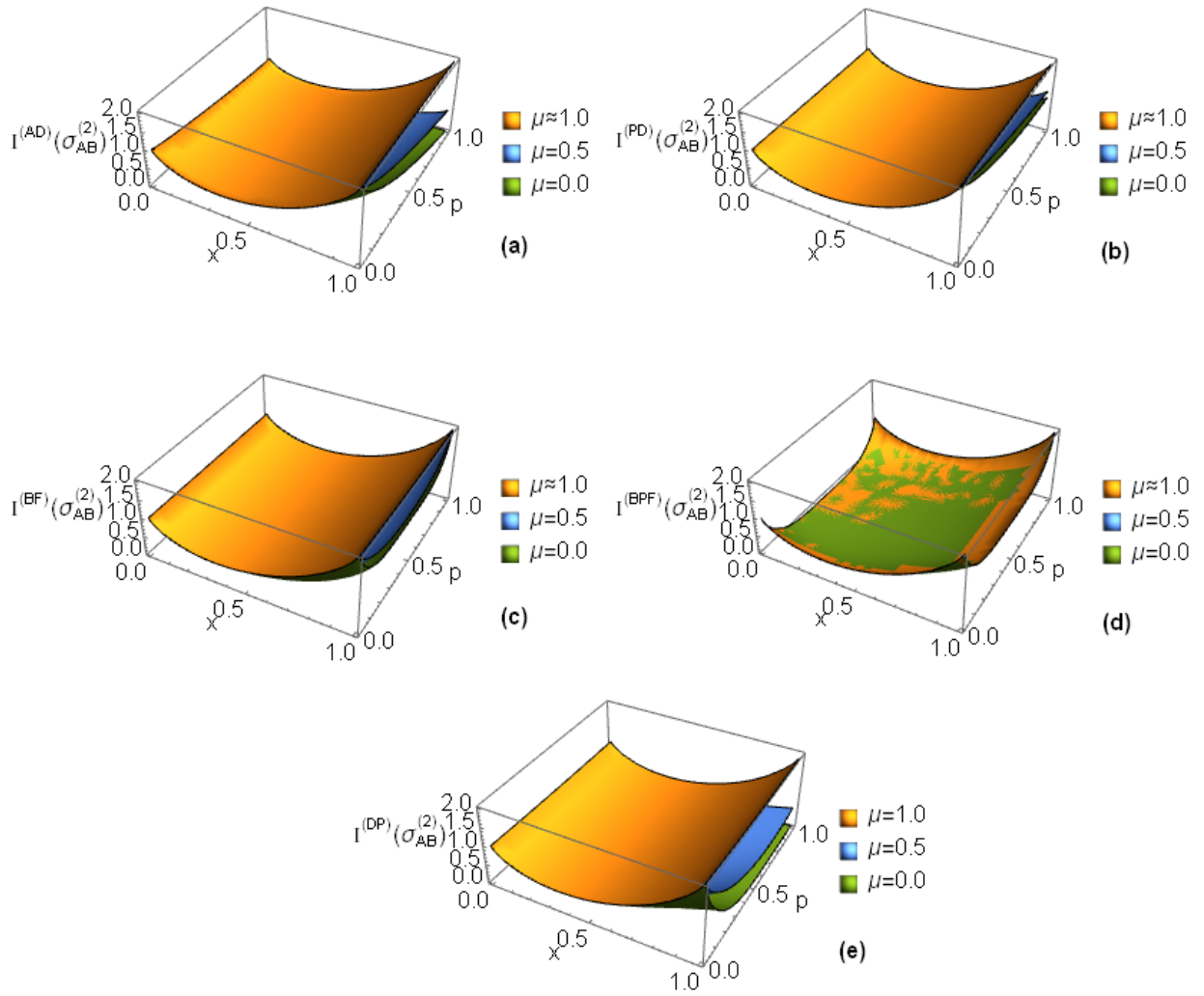


Figure 6. Plots of QMI versus parameters p and x for outputs corresponding to the input $\rho_{AB}^{(2)}$ for some fixed μ . When the channel changes from the memoryless case $\mu = 0$ to long-term memory $\mu = 1$, QMI is enhanced and depending on the some certain values of the parameters, it is maximized for all plots.

4. CONCLUSION

In this present study, we have investigated the dynamical trait of quantum correlations under the two uses of the two-qubit channels with memory constructed by Pauli matrices such as AD, PD, BF, BPF and DP using quantum coherence and QMI as measures of quantum correlations of two 2-qubit systems initially constructed in a quantum state that parameterized. All the observations mention that since the information flows out the system, there is an undeniable decrement of correlations. However, we have observed that for some ranges of the parameter p characterizing the QCs themselves the quantum coherence increases with increasing values of the memory parameter μ especially long-term memory $\mu = 1$. The other significant conclusion is that the coherence and QFI show different behavior for the different input states. On the other hand, since the entanglement is a pivotal resource in the applications of the quantum information and communication processes, by adjusting the parameters and using the different initial states it can relatively be stored to high values as desired in realizing these applications. It would be attractive and meaningful to investigate if the improvement in overall and characteristic behaviors of other correlation measures not considered here could be possible for the considered QCs.

CONFLICT OF INTEREST

The author stated that there are no conflicts of interest regarding the publication of this article.

REFERENCES

- [1] Nielsen M, Chuang IL. Quantum Computation and Quantum Information, 10th Anniversary Ed. Cambridge University Press, Cambridge, 2010.
- [2] DiVincenzo DP. The physical implementation of quantum computation. *Fortschr Phys*, 2000; 48: 771-783.
- [3] Plenio MB, Virmani S. An introduction to entanglement measures. *Quantum Inf Comput* 2007; 7(1): 1-51.
- [4] Breuer HP, Petruccione F. The Theory of Open Quantum Systems, Oxford University Press, U. K.: Oxford, 2002.
- [5] Schlosshauer M. Decoherence and the Quantum-to-Classical Transition, Berlin, Germany: Springer, 2008.
- [6] Xu JS, Xu XY, Li CF, Zhang CJ, Zou XB, Guo GC. Experimental investigation of classical and quantum correlations under Decoherence. *Nat Commun* 2010; 1:7.
- [7] Caruso F, Giovannetti V, Lupo C, Mancini S. Quantum channels and memory effects. *Rev Mod Phys* 2014; 86, 1203.
- [8] Baumgratz T, Cramer M, Plenio MB. Quantifying coherence. *Phys Rev Lett* 2014; 113: 140401.
- [9] Åberg J. Quantifying Superposition. arXiv:0612146v1.
- [10] Glauber RJ. Coherent and Incoherent states of the radiation field. *Phys Rev* 1963; 131: 2766.
- [11] Sudarshan ECG. Equivalence of semiclassical and quantum mechanical descriptions of statistical light beams. *Phys Rev Lett* 1963; 10: 277.
- [12] Harrow AW, Montanaro A. Quantum computational supremacy. *Nature* 2017; 549: 203-209.
- [13] Streltsov A, Adesso G, Plenio MB. Colloquium: Quantum coherence as a resource. *Rev Mod Phys* 2017; 89: 041003.
- [14] Rana S, Parashar P, Lewenstein M. Trace-distance measure of coherence. *Phys Rev A* 2016; 93: 012110.
- [15] Hu ML, Hu X, Peng Y, Zhang YR, Fan H. Quantum coherence and geometric quantum discord. *Physics Reports* 2018; 762-764: 1-100.
- [16] Xi Z, Li Y, Fan H. Quantum coherence and correlations in quantum system. *Sci Rep* 2015; 5: 10922.
- [17] Korzekwa K, Lostaglio M, Oppenheim J, Jennings D. The extraction of work from quantum coherence. *New J Phys* 2016; 18: 023-045.

- [18] Narasimhachar V, Gour G. Low-temperature thermodynamics with quantum coherence. *Nat Commun* 2015; 6: 7689.
- [19] Lostaglio M, Jennings D, Rudolph T. Description of quantum coherence in thermodynamic processes requires constraints beyond free energy. *Nat Commun* 2015; 6: 63-83.
- [20] Joo J, Munro WJ, Spiller TP. Quantum metrology with entangled coherent states. *Phys Rev Lett* 2011; 107: 083601.
- [21] Giovannetti V, Lloyd S, Maccone L. Advances in quantum metrology. *Nature Photon* 2011; 5: 222-229.
- [22] Chuang IL, Vandersypen LMK, Zhou X, Leung DW, Lloyd S. Experimental realization of a quantum algorithm. *Nature* 1998; 393: 143-146.
- [23] Gershenfeld NA, Chuang IL. Bulk spin-resonance quantum computation. *Science* 1997; 275: 350-356.
- [24] Henao I, Serra RM. Role of quantum coherence in the thermodynamics of energy transfer. *Phys. Rev E* 2018; 97: 062105.
- [25] Lloyd S. Quantum coherence in biological systems. *J Phys Conf Ser* 2011; 302: 012037.
- [26] Lambert N, Chen YN, Cheng YC, Li CM, Chen GY, Nori F. Quantum biology. *Nature Physics* 2013; 9: 10-18.
- [27] Gauger EM, Rieper E, Morton JJJ, Benjamin SC, Vedral V. Sustained quantum coherence and entanglement in the avian compass. *Phys Rev Lett* 2011; 106: 040503.
- [28] Duran D. Action in Hamiltonian Models Constructed by Yang-Baxter Equation: Entanglement and Measures of Correlation. *Chin J Phys* 2020; 68: 426-435.
- [29] Groisman B, Popescu S, Winter A. Quantum, classical, and total amount of correlations in a quantum state. *Phys Rev A* 2005; 72: 032317.
- [30] Stinespring WF. Positive functions on C*-algebras. *Proc Am Math Soc*, 1955; 6: 211-216.
- [31] Kraus K. *Effects and Operations: Fundamental Notions of Quantum Theory*, Lecture Notes in Physics, Berlin: Springer, 1983.
- [32] Macchiavello C, Palma GM. Entanglement-enhanced information transmission over a quantum channel with correlated noise. *Phys Rev A*, 2002; 65: 050301(R).
- [33] Yeo Y, Skeen A. Time-correlated quantum amplitude-damping channel. *Phys Rev A* 2003; 67: 064301.
- [34] Winter A, Yang D. Operational Resource Theory of Coherence. *Phys Rev Lett* 2016; 116: 120404.
- [35] Yu CS. Quantum coherence via skew information and its polygamy. *Phys Rev A* 2017; 95: 042337.